

Cite this article as: Feng Qing, Wang Kuishe, Xue Jianchao, et al. Improving Electrocatalytic Activity of IrO₂-Ta₂O₅ Electrode for Oxygen Evolution in Sulfuric Acid Solution by Mn-doping[J]. Rare Metal Materials and Engineering, 2022, 51(08): 2810-2815.

ARTICLE

Improving Electrocatalytic Activity of IrO₂-Ta₂O₅ Electrode for Oxygen Evolution in Sulfuric Acid Solution by Mn-doping

Feng Qing^{1,2}, Wang Kuishe¹, Xue Jianchao^{1,2}, Jia Bo², Hao Xiaojun², Song Kexing³

¹Xi'an University of Architecture and Technology, Xi'an 710055, China; ²Xi'an Taijin Industrial Electrochemical Technology Co., Ltd, Xi'an 710016, China; ³Henan University of Science and Technology, Luoyang 471000, China

Abstract: IrO₂-Ta₂O₅-MnO_x electrodes with different Mn contents were prepared. The effect of Mn content on the physical and electrochemical characteristics of these electrodes was revealed. The results show that the coated IrO₂-Ta₂O₅-MnO_x layer has a larger specific surface area due to its bumpy and porous structure. The doping of a small amount of Mn inhibits the crystallization of the active ingredient IrO₂ and turns it into Ir³⁺. With properly replacing Ir with Mn, the electrocatalytic performance of the IrO₂-Ta₂O₅-MnO_x electrodes can be enhanced dramatically. The increased electrocatalytic activity, longer lifetime and lower cost benefit from the larger active surface area of the Mn-doped electrode, thus promoting the release of oxygen in the sulfuric acid solution.

Key words: oxygen evolution reaction; IrO₂-Ta₂O₅ anode; manganese; electrochemical behavior

With excellent electrochemical performance and long service life, titanium-based precious metal insoluble anodes are widely used in electrochemical industries^[1-5], such as the electrolysis of water, chlor-alkali production, wastewater treatment, metal electrodeposition, and organic synthesis. Previous studies indicate that the oxygen evolution reaction (OER) activity of hydrous and amorphous IrO₂ is much better than that of crystalline and thermally prepared IrO₂^[6]. Srinivasan^[7] attributed the high OER activity of hydrous IrO₂ to the bulk defects within the catalytic material. Later, it is found that the lower calcination temperature of the pyrolytic Ir-oxide can also increase its OER activity^[8]. In 2011, Zhang et al^[9] found that the electrocatalytic activity on the Ti/IrO₂-SiO₂ electrodes is improved significantly by the introduction of silica, which leads to the change in the surface states of active oxide. Then Pascuzzi et al^[10] found that Mn has an impact on the electronic structure of rutile IrO₂ and the electrocatalytic performance is significantly improved by the addition of Mn.

So far, many researches have focused on improving the performance of the iridium-tantalum anode, because of the increasing demand for high current density (6000~8000 A/m²) in the electrolytic production of copper foil. Meanwhile, for

saving cost, mixed-metal-oxide anodes were proposed. For example, Alanazi^[11] found that cobalt doped IrO₂-Ta₂O₅ coating with dense nature coating can extend the life of the IrO₂-Ta₂O₅ anode. The SnO₂-IrO₂-Ta₂O₅ electrode prepared by sol-gel method also shows improved electrocatalytic performance^[12]. Besides, depositing MnO₂ on the Ti/IrO₂-Ta₂O₅ electrode surface is beneficial to decrease the overvoltage for oxygen evolution in pure sulfuric acid^[13].

In this work, the Ti/IrO₂-Ta₂O₅-MnO_x electrode was prepared by introducing Mn to replace Ir. Moreover, the electrocatalytic activity of Ti/IrO₂-Ta₂O₅-MnO_x composite electrodes for oxygen evolution in sulfuric acid solution was also investigated by kinetics method, so as to clarify the positive effects of Mn-doping on these electrodes.

1 Experiment

The Ti/IrO₂-Ta₂O₅-MnO_x electrodes were prepared by dissolving H₂IrCl₆·4H₂O (99.95%, Alfa Aesar), TaCl₅ (Sigma-Aldrich, Budapest, Hungary) and MnCl₂ (98, Sigma-Aldrich) in absolute n-butyl alcohol. The Ir:Ta:Mn atomic ratios selected were 7:3:0, 7:3:0.5, 7:3:1.5, 7:3:2.5, 7:3:3.5. The sample was marked as Mn_x in which atomic percentage of Mn is represented by *x*. The total loading of IrO₂-Ta₂O₅-MnO_x oxide

Received date: March 29, 2022

Foundation item: National Key Research and Development Program of China (2021YFB3400800)

Corresponding author: Wang Kuishe, Professor, Xi'an University of Architecture and Technology, Xi'an 710055, P. R. China, Tel: 0086-29-82202827, E-mail: wangkuishe123@xauat.edu.cn

Copyright © 2022, Northwest Institute for Nonferrous Metal Research. Published by Science Press. All rights reserved.

coating is 2 mg/cm^2 . The calcination temperature of these samples is $500 \text{ }^\circ\text{C}$.

The phases of $\text{IrO}_2\text{-Ta}_2\text{O}_5$ and $\text{IrO}_2\text{-Ta}_2\text{O}_5\text{-MnO}_x$ oxide coatings were determined by X-ray diffraction (XRD) with $\text{Cu K}\alpha$ radiation (Smartlab, Rigaku). The morphology and elements were represented by scanning electron microscopy (JSM IT300). The element chemical state of these samples was collected by X-ray photoelectron spectroscopy (XPS, Axis Ultra, Kratos Analytical Ltd).

The electrochemical workstation (CHI 660E) was employed for electrochemical measurement. The electrolyte used in the tests was $0.5 \text{ mol}\cdot\text{L}^{-1} \text{ H}_2\text{SO}_4$. Saturated Ag/AgCl , platinum and prepared $\text{IrO}_2\text{-Ta}_2\text{O}_5\text{-MnO}_x$ were used as reference electrode, counter electrode and working electrode, respectively. Cyclic voltammetry (CV) test was carried out in the potential range of $0.3\text{--}1.3 \text{ V}$ with the rate of $20 \text{ mV}\cdot\text{s}^{-1}$. The electrochemical impedance spectroscopy (EIS) test was carried out with the output potential of 1.35 V , the amplitude of 5 mV and the frequency range of $1.0^2\text{--}10^5 \text{ Hz}$.

Accelerated lifetime test adopted the $1 \text{ mol}\cdot\text{L}^{-1}$ sulfuric acid system as experimental environment with electrolyte temperature of $60 \text{ }^\circ\text{C}$ and the current density of $4 \text{ A}\cdot\text{cm}^{-2}$. Generally, the accelerated lifetime test ends when anode's voltage was increased to 5 V .

2 Results and Discussion

2.1 XRD analysis

The XRD patterns of all $\text{IrO}_2\text{-Ta}_2\text{O}_5\text{-MnO}_x$ coatings are shown in Fig. 1. We cannot find any diffraction peaks associated with MnO_2 in $\text{IrO}_2\text{-Ta}_2\text{O}_5\text{-MnO}_x$ coatings, which implies that manganese dioxide exists in an amorphous state at this temperature. The peaks observed at 28.02° , 34.7° , 40.05° and 54.01° are related to the rutile IrO_2 . As shown in Fig. 1, the IrO_2 peaks shift to higher diffraction angles with the introduction of Mn cations. The reason is that one atom of Mn

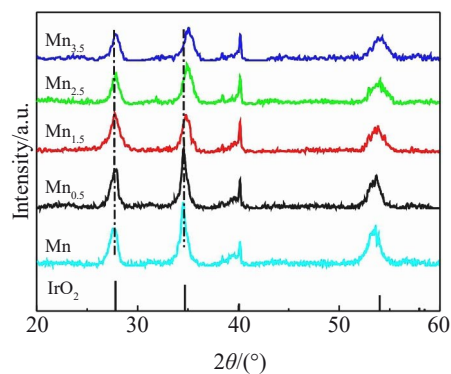
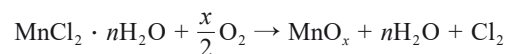
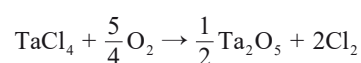
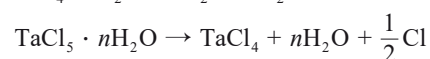


Fig.1 XRD patterns of Ti-supported catalysts Mn_x samples

is marginally smaller than one atom of Ir due to ionic radii difference between iridium (0.0625 nm) and manganese (0.053 nm). In the anode prepared by Mn, Mn replaces Ir of different valence states^[13]. We analyzed the intensity of rutile IrO_2 diffraction peak by XRD pattern. With the increase of MnO_x content, the intensity of IrO_2 diffraction peak in $\text{IrO}_2\text{-Ta}_2\text{O}_5\text{-MnO}_x$ electrode is weaker than that of $\text{IrO}_2\text{-Ta}_2\text{O}_5$ electrode, which indicates that the active ingredient IrO_2 exists in the electrode oxide coating in an amorphous structure. The preparation mechanism of anode thermal decomposition is shown as follows:



2.2 Surface morphology

Fig. 2 indicates that the surface morphology of $\text{IrO}_2\text{-Ta}_2\text{O}_5\text{-}$

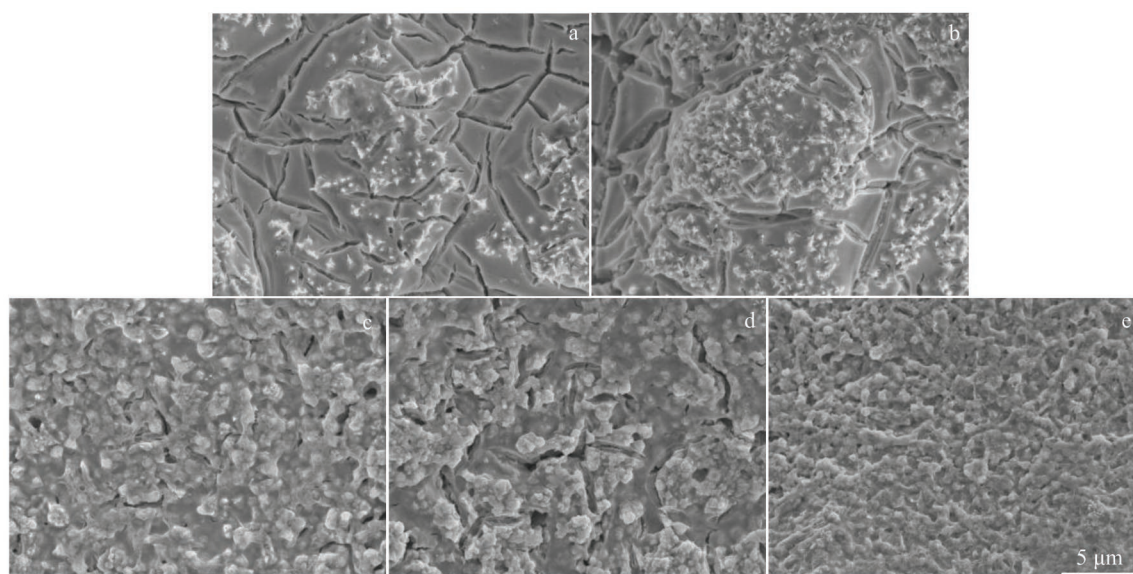


Fig.2 SEM morphologies of Mn_x sample: (a) $\text{Mn}_{0.5}$, (b) $\text{Mn}_{0.5}$, (c) $\text{Mn}_{1.5}$, (d) $\text{Mn}_{2.5}$, and (e) $\text{Mn}_{3.5}$

MnO_x coatings is affected by the content of Mn. In Fig.2a and 2b, IrO₂-Ta₂O₅ electrode shows a dense structure and contains few dispersed needle-like crystals. While as the Mn content increases, the electrodes become porous (Fig. 2c~2e). As shown in Table 1, the result suggests that IrO₂-Ta₂O₅-MnO_x electrode consists of Ir, Ta, O and Mn elements via EDS. Compared with the elements of the IrO₂-Ta₂O₅ electrode, the result indicates that Mn is successfully introduced into the coatings of IrO₂-Ta₂O₅. With the introduction of manganese element, the precipitation of iridium dioxide crystal clusters as well as cracks on the surface of the coating gradually decreases. And thus, a porous surface structure forms.

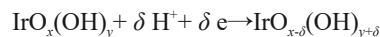
2.3 XPS analysis

Fig.3 indicates electronic state of electrode surfaces. In the electrode of IrO₂-Ta₂O₅, the characteristic peaks of Ta, Ir, C, O, and Mn were analyzed. The binding energies of C 1s peak are calibrated at 284.8 eV (Fig. 3a). High-resolution XPS spectra of O 1s of the five electrodes are shown in Fig.3b. Due to the weak physical adsorption of adsorbed bulk oxygen and/or oxygen-bonded substances on the electrode surface (such as hydroxyl and water)^[2], adsorbed oxygen is formed. The high binding energy of 531.2~531.6 eV may be related to the redox reaction at electrode/water. Freakley et al^[14] proposed a model in 2017 and we used it to fit the XPS spectra of the Ir

4f region (Fig. 3c~3g). As Mn increases, Ir 4f peaks are broader, which means that Ir exists in different oxidation states. Ir³⁺ taken from IrO₂-Ta₂O₅-MnO_x samples increases with the increasing of Mn^[14]. Ir³⁺ exists on the surface with the oxygen vacancies in amorphous IrO₂. In addition, it is believed that the activity of amorphous IrO₂ is better than that of crystalline IrO₂^[15]. The oxidation state of Mn was also investigated by XPS. According to Ref.[16], the 2p peak value of Mn gradually shifts to a high value as the valence state of Mn increases. Based on the XRD and XPS results, we can conclude that Mn is partially inserted as Mn³⁺ and Mn⁴⁺ in rutile IrO₂.

2.4 Electrochemical performance

Fig. 4a shows the typical CV curves of IrO₂-Ta₂O₅-MnO_x electrodes with different contents of Mn. The current redox transformation of active oxides and the surface charging occur in the potential range of 0.3~1.3 V. As shown in Fig. 4a, the shape of all the CV curve is similar, the redox transition of Ir(III)/Ir(IV) and Ir(IV)/Ir(V) solid-state^[17] and proton exchange forms two pairs of broad redox transition peaks (0.4~0.8 V). The formula of these reactions is as follows:



Accordingly, the voltametric charge (q^*), which is positively correlated with the number of active sites, can be characterized by integrating the area of the CV curve^[18]. When the Mn content increases, it shows that q^* first increases when Mn content reaches the maximum of Mn_{2.5} and then decreases. The increase of q^* is caused by surface physical structure with more pores.

The electrodes' apparent electrocatalytic activity is measured based on the anodic polarization curves. Fig.4b shows that the apparent electrocatalytic activity of the IrO₂-Ta₂O₅-MnO_x coatings increases as the Mn content rises, and then it decreases when the Mn content is higher than 2.5at%. The

Table 1 Elemental composition of Mn_x samples (wt%)

Sample	Ir	Ta	O	Mn
Mn _{0.0}	47.89	26.92	25.19	-
Mn _{0.5}	50.49	24.05	24.46	1.00
Mn _{1.5}	50.95	20.22	25.12	3.71
Mn _{2.5}	51.75	19.50	23.91	4.84
Mn _{3.5}	51.72	16.35	25.21	6.72

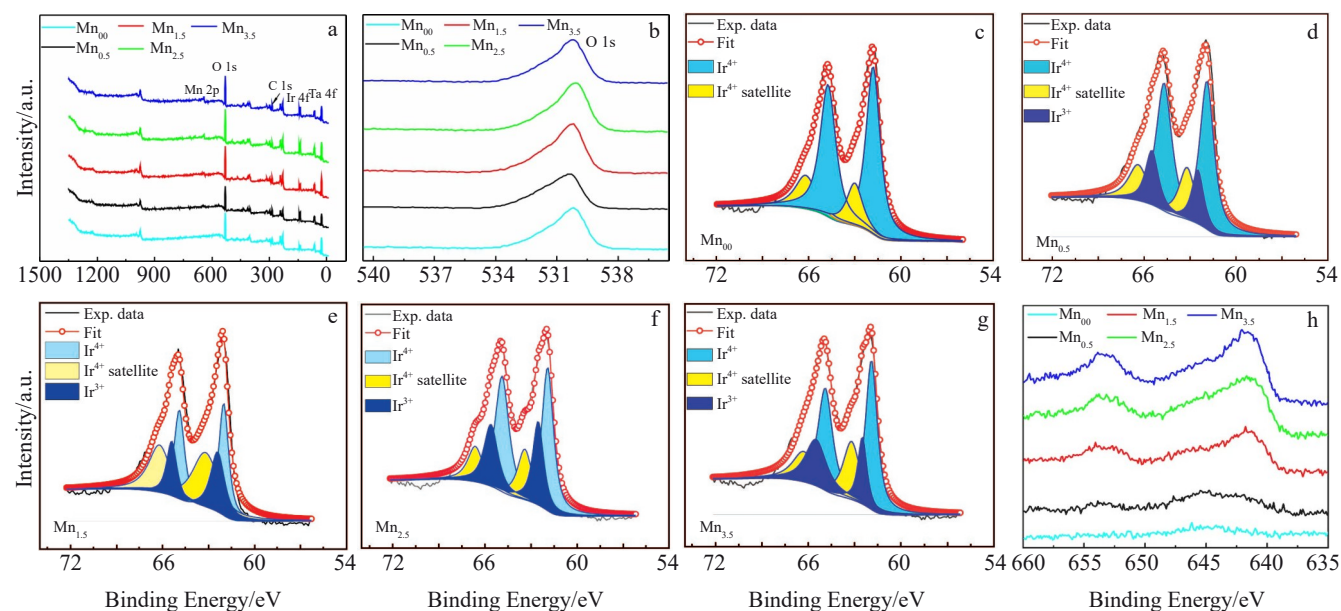


Fig.3 XPS spectra of Mn_x samples: (a) survey spectra, (b) O 1s spectra, (c~g) Ir 4f spectra, and (h) Mn 2p spectra

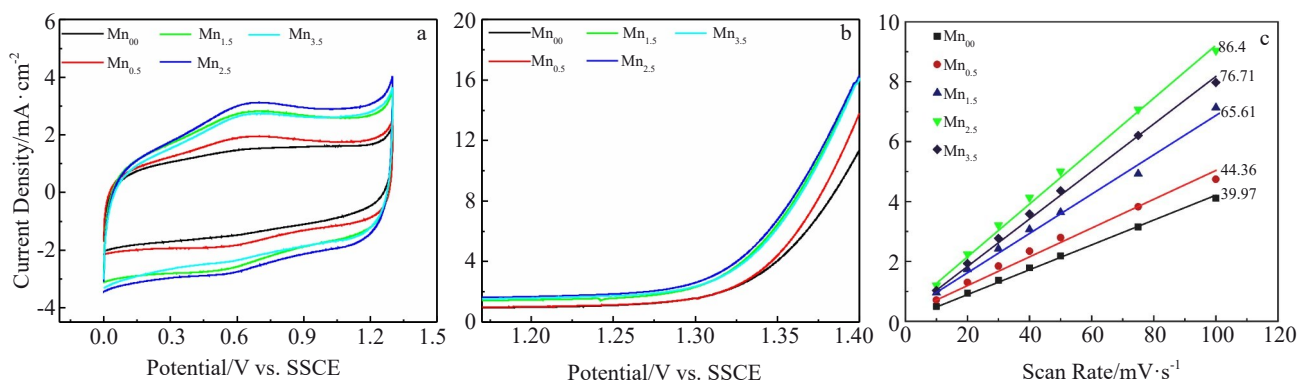
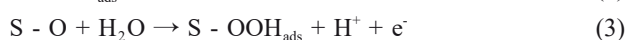
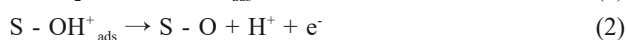
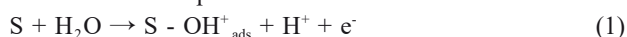


Fig.4 Electrochemical performance of the electrodes with different Mn contents: (a) CV curves, (b) linear sweep voltammetry curves, and (c) ECSA plots

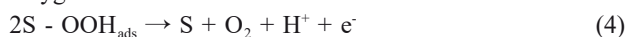
anodes have more active sites because of the porous structure and the amorphous of IrO_2 . Therefore, the electro-catalytic activity on OER reaches the peak when the addition content of Mn is 2.5at%. It is well known that the electrochemically active surface area (ECSA) of electro-catalysts can be expressed in terms of double-layer capacitance ($2C_{dl}$). The calculated ECSA value of the $\text{Mn}_{2.5}$ sample is $172.8 \text{ mF}\cdot\text{cm}^{-2}$, which is much larger than $79.94 \text{ mF}\cdot\text{cm}^{-2}$ of the Mn_{00} sample. This indicates that the introduction of Mn promotes the increase of the active area of the titanium anode, and the higher ECSA value is the key factor for the high catalytic activity of $\text{Mn}_{2.5}$.

The electrochemical behavior of the prepared $\text{IrO}_2\text{-Ta}_2\text{O}_5\text{-MnO}_x$ electrodes is obtained by fitting the experimental data of IR-corrected Tafel curve. The characteristics of OER on the $\text{IrO}_2\text{-Ta}_2\text{O}_5$ and $\text{IrO}_2\text{-Ta}_2\text{O}_5\text{-MnO}_x$ electrodes are shown in Fig.5a. Two lines segment in the figure represent the low- and high-overpotential. A secondary position on the Tafel area is the Tafel plots of the IrO_2 -based catalysts with higher current density. The result suggests that both low-overpotential and high-overpotential Tafel slopes increase with raising the Mn content, and then decrease when the addition content of Mn is higher than 2.5at%. The slope changes by the electrochemical reaction mechanism variations. In the detailed mechanism steps^[19-21], the water molecules in the electrolyte first interact with the S site to form the HO_{ads} intermediate (Eq.(1)). The HO_{ads} is then deprotonated into the S-O by an accompanying single-electron transfer process (Eq.(2)). The S-O intermediate further reacts with water to form adsorbed HOO_{ads} at site S (Eq.(3)), which in turn generates O_2 and releases site S (Eq.(4)). The reaction mechanism for OER mainly consists of the following steps^[22].

Kinetic control steps:



Oxygen evolution:



In above Kinetic control steps (Eq.(1~3)), the Tafel slope values which represent the rate-determining step (RDS) are 120, 60 and 40 mV/dec, respectively^[22]. In contrast, the slope

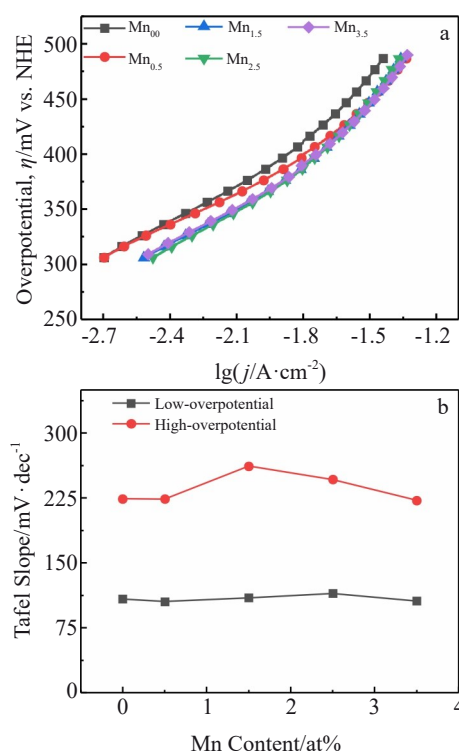


Fig.5 Tafel lines (a) and Tafel slopes (b) of the electrodes measured in low-overpotential and high-overpotential areas as a function of Mn content

values of the $\text{IrO}_2\text{-Ta}_2\text{O}_5$ electrodes and $\text{IrO}_2\text{-Ta}_2\text{O}_5\text{-MnO}_x$ electrodes are higher. It shows that OER occurs more difficultly on $\text{IrO}_2\text{-Ta}_2\text{O}_5\text{-MnO}_x$ electrodes than on $\text{IrO}_2\text{-Ta}_2\text{O}_5$ electrodes.

In the test of oxygen evolution reaction (1.35 V, H_2SO_4 solution), the electrode surface characteristic and electrochemical behavior were investigated by EIS. As shown in Fig.6, the value of impedance spectra of $\text{IrO}_2\text{-Ta}_2\text{O}_5\text{-MnO}_x$ electrodes is reduced as the increase of Mn content, indicating that the electrocatalytic activity for OER is improved. In Fig.6a, the small semicircle in high frequency represents that the film process occurs in the tracks of the coating. The large semicircle in low frequency represents the charge-transfer process at the electrode/electrolyte interface. And the

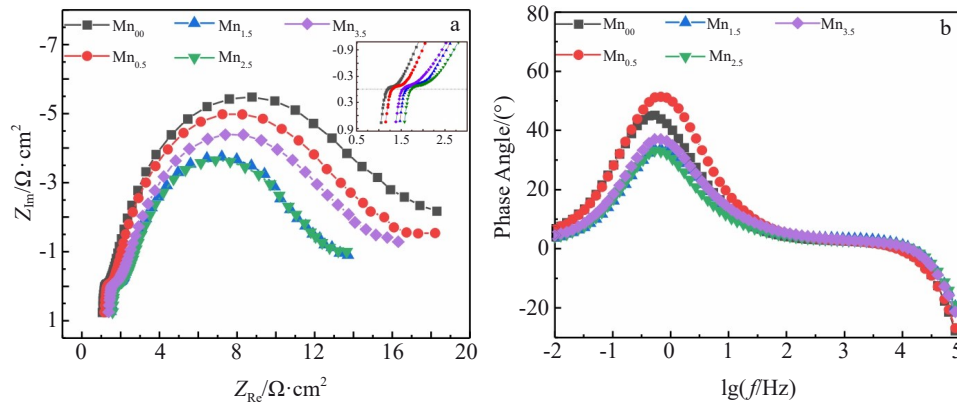


Fig.6 EIS plots of the electrodes with different Mn contents: (a) Nyquist diagrams and (b) Bode plots (Z is impedance)

amorphous semicircle in intermediate frequency is thought to be related to the porous characteristics of the thermal prepared active oxide layer. Fig. 6b displays that the characteristic of high frequency inductive is caused by the coating's porous structure.

2.5 Electrocatalytic stability

Fig. 7 illustrates the accelerated lifetime of the $\text{IrO}_2\text{-Ta}_2\text{O}_5$ electrodes with different contents of Mn. When the content of Mn is 1.5at%, the longest lifetime of 20 d is obtained. Electrode deactivation occurs possibly due to the following three factors: erosion, corrosion and support passivation^[23]. Erosion occurs in the early stage of the anodization experiment, and the formation of strong bubbles leads to the separation of loosely bound particles. The dissolution of the active material of the anode coating is the major mechanism of the failure of the anode. For example, the organic material usually reacts with the active material, and Ir^{4+} is oxidized to IrO_4^{2-} at high overpotentials. The coating with multiple cracks and pores is easy to form oxygen diffusion channels, which causes the passivation of Ti substrate as well as the increasing of anode potential, so as to complete deactivation of the anode. It can be attributed to the formation of a non-conductive TiO_2 layer on the surface of the titanium substrate. The oxidation of the titanium support largely depends on the degree of protection provided by the oxide coating. On the one hand, the lifetime of the electrodes (Fig. 7) is associated with the amorphous structure of the coatings. Amorphous IrO_2

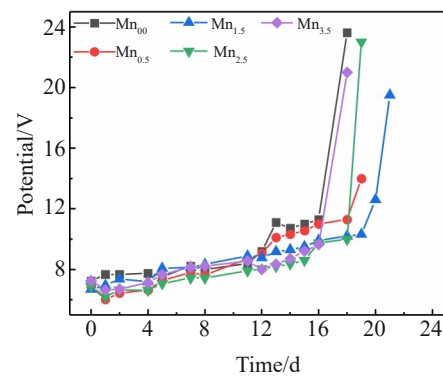


Fig.7 Accelerated lifetime of the $\text{IrO}_2\text{-Ta}_2\text{O}_5\text{-MnO}_x$ electrodes in 1 mol/L H_2SO_4 solution at a current density of 4 A/cm^2

compared with crystallized IrO_2 is less stable during the electrocatalytic process. As a result, amorphous IrO_2 dissolves faster in the reaction. On the other hand, the lifetime also depends on the surface morphology with a high MnO_x content. The mechanical rupture of the coating occurs at high pressure. And the occurrence of cracks leads to the formation of oxygen diffusion channels, leading to passivation of the substrate. Table 2 shows a comparison of the service lifetimes of different electrodes under sulfuric acid solution. Clearly, the $\text{Ti/IrO}_2\text{-Ta}_2\text{O}_5\text{-MnO}_x$ electrode has a higher service lifetime than other electrodes under similar or worse conditions.

Table 2 Service lifetime comparison of different electrodes

Electrode	Electrolyte	Current density/ $\text{A}\cdot\text{m}^{-2}$	Service lifetime/h	Tafel slope	Ref.
$\text{IrO}_2\text{-Ta}_2\text{O}_5\text{-CNT}$	1 mol/L H_2SO_4	4	400	-	[24]
$\text{IrO}_2\text{-Ta}_2\text{O}_5\text{-MWCNT}$	1 mol/L H_2SO_4	2.5	120	113	[25]
$\text{IrO}_2\text{-Ta}_2\text{O}_5\text{-TiO}_2$	2 mol/L H_2SO_4	1	~110	-	[26]
$\text{IrO}_2\text{-Ta}_2\text{O}_5$	1 mol/L H_2SO_4	2	500	-	[27]
$\text{IrO}_2\text{-Ta}_2\text{O}_5\text{-Mn}$	1 mol/L H_2SO_4	4	504	105	This work

3 Conclusions

1) A non-precious metal Mn-doped IrO₂-Ta₂O₅ anode can be prepared by thermal decomposition, and a series of analysis and characterization of its surface morphology, electrochemical performance and stability show that the introduction of Mn element can better balance the relationship between them.

2) In addition, the doped Mn element replaces part of Ir position in IrO₂, forming a uniform solid solution, leading to the formation of Ir³⁺ and obtaining Ir³⁺/Ir⁴⁺ electron pairs, thereby improving the redox performance of the anode. At the same time, with the increase of Mn content, the anode presents an uneven and porous structure, which contributes to the increase of the specific surface area of the anode and promotes the exposure of active sites.

3) The addition of an appropriate amount of Mn element can well control the surface morphology of the anode, reduce cracks, and contribute to the prolongation of life. On the premise that the stability is not affected, the introduction of Mn can effectively reduce the loading of Ir (33.3%), realize the substitution of base metal elements for noble metals, and it is beneficial to expand the scope of anode industrial application.

References

- Trasatti S. *Electrochimica Acta*[J], 2000, 45(15): 2377
- Wei Z, Kang X Q, Xu S Y et al. *Chinese Journal of Chemical Engineering*[J], 2021, 32(4): 191
- Hu J M, Zhang J Q, Cao C N. *International Journal of Hydrogen Energy*[J], 2004, 29(8): 791
- Feng Y, Li J, Wang X et al. *International Journal of Hydrogen Energy*[J], 2010, 35(15): 8049
- Park S R, Park J S. *Journal of the Korean Chemical Society*[J], 2020, 23(1): 1
- Geiger S, Kasian O, Shrestha B R et al. *Journal of the Electrochemical Society*[J], 2016, 163(11): 3132
- Srinivasan S G. *Journal of Electroanalytical Chemistry and Interfacial Electrochemistry*[J], 1978, 86(1): 89
- Reier T, Teschner D, Lunkenbein T et al. *Journal of the Electrochemical Society*[J], 2014, 161(9): 876
- Zhang J J, Hu J M, Zhang J Q et al. *International Journal of Hydrogen Energy*[J], 2011, 36(9): 5218
- Pascuzzi M, Hofmann J P, Hensen E. *Electrochimica Acta*[J], 2021, 366: 137 448
- Alanazi N M, Al-Abdulhadi A I, Al-Zharani T Y et al. *Surface and Coatings Technology*[J], 2019, 374: 815
- Ardizzone S, Bianchi C L, Cappelletti G et al. *Journal of Electroanalytical Chemistry*[J], 2006, 589(1): 160
- Nijjer S, Thonstad J, Haarberg G M. *Electrochimica Acta*[J], 2001, 46(23): 3503
- Freakley S J, Ruiz-Esquiús J, Morgan D J. *Surface & Interface Analysis*[J], 2017, 49(8): 794
- Verena Pfeifer. *Surface & Interface Analysis*[J], 2016, 48(5): 261
- Biesinger M C, Payne B P, Grosvenor A P et al. *Applied Surface Science*[J], 2011, 257(7): 2717
- Oliveira-Sousa A D, Silva M, Machado S et al. *Electrochimica Acta*[J], 2000, 45(27): 4467
- Silva L A da, Alves V A, Silva M A P da et al. *Canadian Journal of Chemistry*[J], 1997, 75(11): 1483
- Doyle R L, Lyons M E G. *Photoelectrochemical Solar Fuel Production*[M]. Cham: Springer International Publishing, 2016: 41
- Rossmeisl J, Logadottir A, Nørskov J K. *Chemical Physics*[J], 2005, 319(1-3): 178
- Chen F Y, Wu Z Y, Adler Z et al. *Joule*[J], 2021, 5(7): 1704
- Santana M, Faria L, Boodts J. *Journal of Applied Electrochemistry*[J], 2005, 35(9): 915
- Martelli G N, Ornelas R, Fajta G. *Electrochimica Acta*[J], 1994, 39(11-12): 1551
- Fan Y, Xuan C. *Journal of the Electrochemical Society*[J], 2016, 163(8): 209
- Mehdipour M, Tabaian S H, Firoozi S. *Journal of the Iranian Chemical Society*[J], 2021, 18: 233
- Kariman A. *Journal of the Electrochemical Society*[J], 2019, 166(8): 248
- Xu L K, Scantlebury J D. *Corrosion Science*[J], 2003, 45(12): 2729

Mn 掺杂提高 IrO₂-Ta₂O₅ 电极在硫酸溶液中析氧的电催化活性

冯 庆^{1,2}, 王快社¹, 薛建超^{1,2}, 贾 波², 郝小军², 宋克兴³

(1. 西安建筑科技大学, 陕西 西安 710055)

(2. 西安泰金工业电化学技术有限公司, 陕西 西安 710016)

(3. 河南科技大学, 河南 洛阳 471000)

摘 要: 制备了不同 Mn 含量的 IrO₂-Ta₂O₅-MnO_x 电极。揭示了 Mn 含量对该类电极的物理和电化学特性的影响。结果表明, 涂覆的 IrO₂-Ta₂O₅-MnO_x 层由于其凹凸不平的多孔结构而具有较大的比表面积。少量 Mn 的加入抑制了活性成分 IrO₂ 的结晶, 并将其转化为 Ir³⁺。适当地用 Mn 代替 Ir 可以显著提高 IrO₂-Ta₂O₅-MnO_x 电极的电催化性能。高的电催化活性、长的寿命和低的成本得益于 Mn 掺杂的电极具有更大的活性表面积, 从而促进了硫酸溶液中氧的析出。

关键词: 析氧反应; IrO₂-Ta₂O₅ 阳极; 锰; 电化学行为

作者简介: 冯 庆, 男, 1981 年生, 博士, 西安建筑科技大学, 陕西 西安 710055, 电话: 029-86968404, E-mail: fengqing0715@126.com